



HAL
open science

Microrheology of hemolymph plasma of the bumblebee *Bombus terrestris*

Amandine Lechantre, Baptiste Martinet, Véronique Thévenet,
Oune-Saysavanh Souramasing, José Bico, Bérengère Abou

► **To cite this version:**

Amandine Lechantre, Baptiste Martinet, Véronique Thévenet, Oune-Saysavanh Souramasing, José Bico, et al.. Microrheology of hemolymph plasma of the bumblebee *Bombus terrestris*. *Journal of Experimental Biology*, 2023, 226 (14), pp.jeb245894. 10.1242/jeb.245894 . hal-04186386

HAL Id: hal-04186386

<https://hal.science/hal-04186386>

Submitted on 23 Aug 2023

HAL is a multi-disciplinary open access archive for the deposit and dissemination of scientific research documents, whether they are published or not. The documents may come from teaching and research institutions in France or abroad, or from public or private research centers.

L'archive ouverte pluridisciplinaire **HAL**, est destinée au dépôt et à la diffusion de documents scientifiques de niveau recherche, publiés ou non, émanant des établissements d'enseignement et de recherche français ou étrangers, des laboratoires publics ou privés.

Microrheology of hemolymph plasma of the bumblebee *Bombus terrestris*

Amandine Lechantre,^{1,2} Baptiste Martinet,³ Véronique Thévenet,¹
Oune-Saysavanh Souramasing,¹ José Bico,² and Bérengère Abou¹

¹*Matière et Systèmes Complexes, UMR7057 CNRS - Université Paris Cité, 75205 Paris, France*

²*Physique et Mécanique des Milieux Hétérogènes, UMR7636 CNRS, ESPCI Paris, Université Paris Sciences & Lettres & Sorbonne Université, 75005, Paris, France*

³*Université de Mons (UMons), Research institute of Biosciences, Laboratory of Zoology, Place du Parc 20, 7000 Mons, Belgium*

(Dated: June 1, 2023)

Viscosity, which impacts the rate of hemolymph circulation and heat transfer, is one of the transport properties that affects the performance of an insect. Measuring the viscosity of insect fluids is challenging because of the small amount available per specimen. Using particle tracking microrheology, which is well suited to characterise the rheology of the fluid part of the hemolymph, we studied the plasma viscosity in the bumblebee *Bombus terrestris*. In a sealed geometry, the viscosity exhibits an Arrhenius dependence with temperature, with an activation energy comparable to that previously estimated in hornworm larvae estimated in [1]. In an open to air geometry, it increases by 4 to 5 orders of magnitude during evaporation. Evaporation times are temperature dependent and longer than typical insect hemolymph coagulation times. Unlike standard bulk rheology, microrheology can be applied to even smaller insects, paving the way to characterise biological fluids such as pheromones, pad secretions or cuticular layers.

Keywords: Biological fluids, Viscosity, Insect physiology

I. INTRODUCTION

Hemolymph, the counterpart of blood in invertebrates, circulates freely throughout the insect body, bathing all internal tissues. It is composed of a fluid plasma in which are suspended hemocytes, cellular defence units partly responsible for the immune system of insects [2]. Plasma also contains many compounds such as free amino acids or proteins which differ from one insect to another, and potentially between females and males during development. Sugars, such as trehalose, whose function is to provide energy to tissues, are also present [3–6]. Haemolymph plays a major role in the survival and physiology of insects. This circulating fluid transports nutrients, hormones and waste products through the body, maintaining correct humidity, optimal body temperature and body shape [4, 7]. In addition, when the cuticle is damaged, hemolymph coagulates, preventing pathogens from entering the insect body [8, 9].

Among the physical properties that govern the flow of a fluid, viscosity is a key parameter, and it depends on temperature. Unlike mammals, the body temperature of insects varies according to activity and the temperature of the external environment by thermoregulation [10]. These temperature variations directly affect the viscosity of plasma and subsequently hemolymph, and therefore their circulation. Such changes in viscosity have important consequences for insect physiology. Several studies show that, among living beings, insects suffer particularly from the increase in temperature and temperature extremes induced by global warming [10–13]. In addition, studies show that heat waves could have an impact on the body water content of insects such as bumblebees [14, 15]. They would therefore have a direct effect on the viscosity of the plasma of the insect. In this context, probing the influence of temperature on the rheological properties of hemolymph and plasma appears to be crucial.

Because of their small size, insects contain small volumes of fluid. This makes it difficult to collect the fluid and analyse it [16]. Recently, the rheology of plasma and hemolymph has been studied in lepidoptera larvae, but not in adult insects [1, 17]. Kenny *et al.* [1] measured the viscosity in hornworm larvae was measured with a cone and plate viscometer using a volume of 0.7 mL per sample per specimen. These large quantities of fluid can only be collected from large insects, which represent a small fraction of insect species. In general, once the liquid extraction procedure has been implemented, the volume obtained for most insects is too small to perform viscosity measurements with a standard rheometer.

In this context, particle tracking microrheology appears to be a relevant alternative technique. It typically requires 1 μ L of fluid and consists of determining the fluid rheological properties from the Brownian motion of micrometric tracer beads immersed in it. At the micrometre scale, the beads probe the relationship between stress and deformation in their local environment. The technique is well suited to the study of small insects that secrete very small amounts

of fluid, provided that it can be extracted, but also to the study of biological entities, such as living cells [18, 19]. Recent studies on insect footprints or on the cuticular hydrocarbon layer of ants have shown that it is even possible to carry out viscosity measurements with sample volumes of the order of 10 pL [20–22].

In this paper, we present measurements of the plasma viscosity of the common buff-tailed bumblebee *Bombus terrestris* with temperature, using particle tracking microrheology. This technique is particularly useful for the study of the rheological properties of the plasma. In the hemolymph, however, the tracer beads would only probe the suspension medium of the blood cells, the plasma, and not the hemolymph, because the distance between the hemocytes is greater than the size of the tracer beads (1 μm in diameter). A different technique is therefore needed to study the rheology of the whole fluid, the plasma and the blood cells, such as the one used to study hornworm hemolymph [1], which requires larger sample volumes. However, an interesting aspect of the microrheology technique used here for hemolymph is that it can detect spatial heterogeneities in the rheology of the material by analysis of different tracers localised in the sample. It could therefore be used to detect hemolymph coagulation by observing beads immersed in different areas of the sample, whether liquid or gel. This technique could also complement recent measurements using nanorheological magnetic rotational spectroscopy with nanorods, which has allowed the quantitative study of nucleation of cell aggregates during coagulation [17]. In this active microrheology technique, a magnetic torque is applied to 10 μm long nanorods. The response of the material, probed at the nanorod scale, can be probed in the non-linear large deformation regime, and may depend on the amplitude of the magnetic torque. In the clot, for example, the nanorod may destroy the structure under a significant torque and the analysis of the rheological properties may not be straightforward. With our particle tracking technique, in contrast, only the linear regime of small deformation is probed, by thermal agitation of the tracer beads. As they provide information in different deformation regimes and at different length scales, the two techniques are complementary.

Our efforts focused on bumblebees because, among the declining insects, they play a crucial role in the pollination of crops and wild plants in temperate regions and are particularly sensitive to temperature increases [23–25]. The rheology of the bumblebee plasma was studied in two geometries, one open to air and the other sealed. In the sealed geometry, which prevents contamination and evaporation, we compared the plasma viscosity of bumblebees *B. terrestris* with that of hornworm larvae measured by Kenny *et al.* [1]. In open geometry, we measured the evaporation dynamics of the plasma drop as a function of temperature, as well as the associated characteristic evaporation times.

II. MATERIALS AND METHODS

A. Bumblebees

Bumblebees, *Bombus terrestris* (L. 1758), were obtained from the standard product “Masculino system (*Bombus terrestris*)” from Biobest Group NV (Westerlo, Belgium). Only male specimens were selected because their plasma composition is less variable over time than that of females, whose hormonal state varies [23]. Specimens were grouped by 50 in a cardboard box, were all the same age (3 – 4 days) and were fed with liquid sugar supplied by Biobest (Biosweet). Plasma was collected within a week of receipt.

B. Extraction of hemolymph and preparation of plasma samples

A protocol adapted from Arafah *et al.* [26] was used to extract hemolymph from bumblebees. It was collected using a stretched glass capillary with a large tip (external diameter $\sim 50 - 200 \mu\text{m}$), inserted a few millimetres into the insect body to avoid contamination. The fluid was drawn up by capillary effect by placing the glass capillary dorsally under the second tergite of the abdomen (Fig. 1A). Puncturing the dorsal region allows a sufficient quantity of fluid to be collected without injuring the bumblebees. It also avoids perforating the digestive tract, which would be a source of contamination for the sample. Volumes of 20 μL per individual were collected. They were visually clear, providing further confirmation of the absence of contamination from fatty substances, which would have caused a slight haze to form. Batches of fluid from five bumblebees were prepared, dispensed into Eppendorf tubes and sealed under argon gas. In practice, the fluid obtained using this protocol is mainly plasma, with only a few cells suspended. The samples were then left to sediment in the sealed Eppendorf tubes for a few tens of minutes ($\sim 30 - 100\text{min}$) in order to separate the plasma from the few cells present. The supernatant – corresponding to the plasma – was then collected and distributed in 5 μL Eppendorf tubes sealed under argon gas. A small volume of a concentrated aqueous suspension of melamine beads (bead volume fraction 10%, bead diameter 0.88 μm , Granuloshop, Chatou, France) was added to the different plasma batches. The ratio of bead suspension volumes to plasma was calculated to give a volume fraction of beads of less than 1% in each batch. The different batches were stored at -20°C for up to two months (Fig. 1A). Mixing five bumblebee samples allowed us to test the suitability of the technique independently

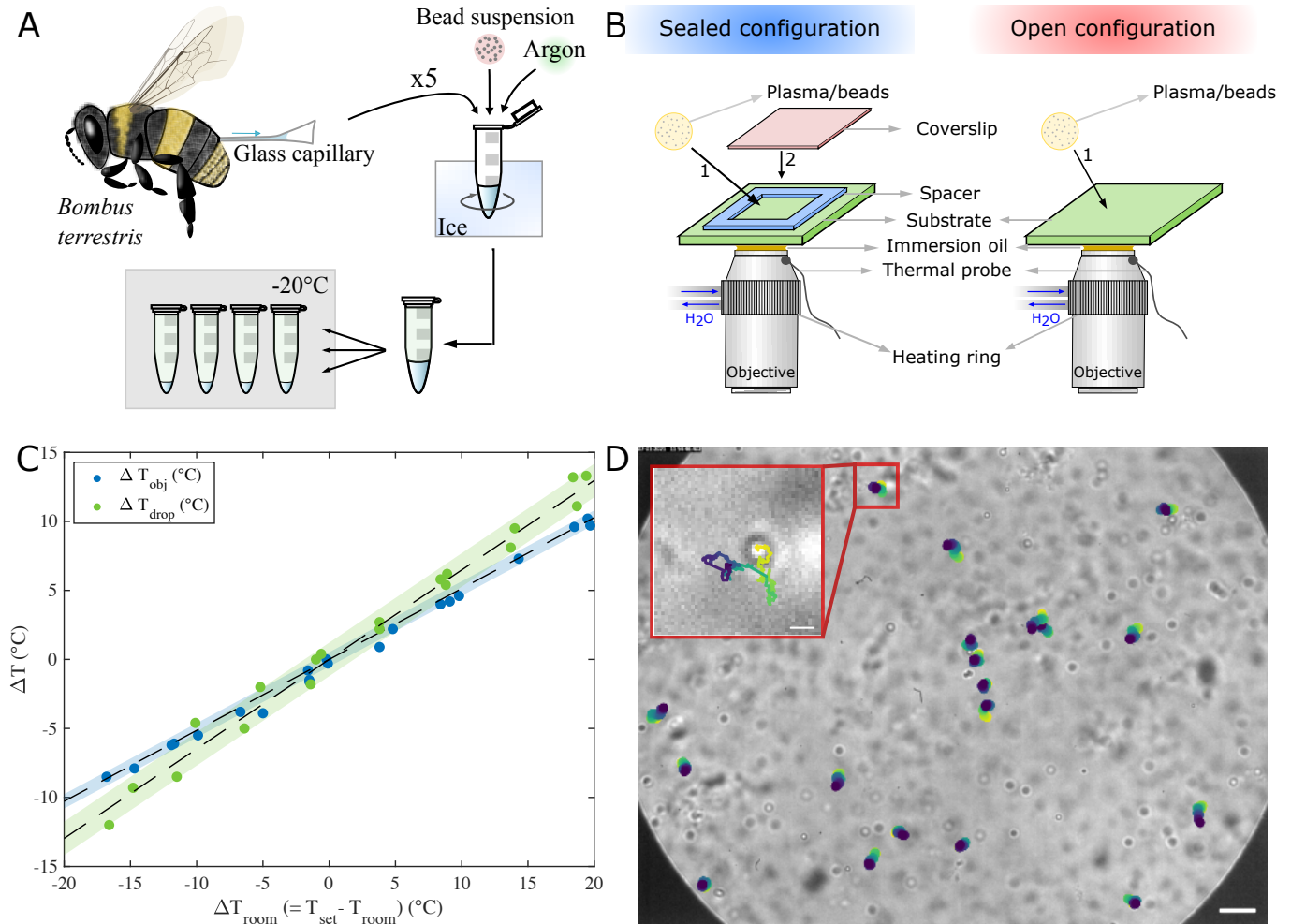


Figure 1. Particle tracking microrheology technique. (A). Principle of plasma extraction from bumblebees and microrheology measurements. The plasma is collected through a stretched capillary tube inserted into the insect body. Plasma samples from 5 specimens are mixed with a small volume of a concentrated aqueous suspension of melamine beads. This mixture is then distributed into $5 \mu\text{L}$ Eppendorf tubes. (B). Sketch of the sealed geometry (left) and the open geometry (right) configurations. A drop of plasma/beads is placed on the microscope slide (1); in the sealed configuration, this is then covered by a coverslip (2). (C). Calibration curves of the sample temperature, ΔT_{drop} (difference between the set temperature and the sample temperature), and the objective temperature, ΔT_{obj} (difference between the set temperature and the objective temperature), as a function of the room temperature ΔT_{room} (difference between the set temperature and the room temperature). The shaded areas highlight the temperature ranges measured with a drop of water as a sample. (D). Tracking of beads over 5 seconds (sealed geometry at 30°C , $\eta = 1.7 \text{ mPa}\cdot\text{s}$). The colour associated with the position of the bead varies over time (from yellow to blue). Scale bar: $10 \mu\text{m}$. Insert: Magnification of the displacement of a bead (scale bar: $1 \mu\text{m}$).

of biological variability, while measuring the general behaviour of bumblebee plasma and limiting the bias associated with variations in composition between individuals. However, the same approach could have been used to measure each sample from the same individual independently.

C. Microrheology

Particle tracking microrheology is a technique that consists of determining the rheological properties of a material from the study of the Brownian motion of micrometric beads embedded in the material (for reviews, see [18, 19]). In our setup, the sample was placed under an inverted microscope (Leica DM IRB, Germany) at $100\times$ magnification (oil immersion, Numerical Aperture 1.3), and the Brownian motion of the micrometric beads was measured with a high-speed sCMOS camera (EoSens Mikrotron, Photon Lines, Pacé, France). Below we describe the two working

geometries in which the samples were studied, the temperature control system of the sample, and finally the analysis of the Brownian motion, which enables the determination of the rheological properties of the material.

1. Working geometry and temperature control

Two working geometries, referred to as *sealed* and *open*, were used to study the rheological properties of the plasma. In the sealed geometry, which prevents contamination or evaporation, a volume of $2.5\ \mu\text{L}$ of plasma was deposited on a microscope slide and a microscope coverslip was placed over the top, separated by a thin adhesive spacer of dimension $1\ \text{cm} \times 1\ \text{cm} \times 250\ \mu\text{m}$ (Gene frame $\text{\textcircled{R}}$, VWR International, France) (Fig. 1B, left). In the open geometry, where a $3\ \mu\text{L}$ drop of plasma was deposited on a microscope slide and left in the open air (Fig. 1B, right). Before depositing the plasma drop in the working geometry, the Eppendorf tubes were thawed at room temperature and stirred for a few seconds to disperse the beads evenly throughout the sample.

The microscope objective was equipped with a laboratory-designed heating ring which includes a water circulation controlled by a thermostat to within $\pm 0.3^\circ\text{C}$. The temperature of the plasma drop could thus be adjusted through the objective heating ring via the immersion oil in contact with the sample, as shown in Fig. 1B. A peristaltic micro-pump ensured a continuous exchange of water between the thermostat and the heating ring.

To predict the temperature of our plasma droplet samples with our device, calibration curves were established with water droplets whose temperature was directly measured with an internally positioned thermocouple probe. Fig. 1C displays the evolution of ΔT_{obj} ($= T_{set} - T_{obj}$) and ΔT_{drop} ($= T_{set} - T_{drop}$) with ΔT_{room} ($= T_{set} - T_{room}$), where T_{set} is the temperature of the thermostatic bath, T_{obj} the temperature of the objective measured just below the sample and T_{drop} , the temperature of a water droplet (Fig. 1B). These calibration experiments allowed us to establish the following calibration laws to be used with the plasma droplets in the microrheology experiments: $\Delta T_{drop} = 0.65\Delta T_{room} \pm 1.21^\circ\text{C}$ and $\Delta T_{obj} = 0.51\Delta T_{room} \pm 0.52^\circ\text{C}$.

2. Brownian motion analysis

Once the plasma droplet was deposited in the working geometry and thermalization was effective, the Brownian motion of the tracer beads in the droplet was recorded for 20 s at 100 frames per second (fps) with the high-speed camera under the inverted microscope. The positions $x_i(t)$ and $y_i(t)$ of each bead near the focal plane (typically between 15 and 30 beads depending on the realization) were tracked with image analysis software developed locally under ImageJ [27]. The beads close to the surfaces – the microscope slide and the free surface of the drop – were not selected in order to avoid measurement biases due to the friction of the probe near a surface. For each tracer bead i , the time-averaged mean-squared displacement was calculated from the successive positions x_i and y_i between time t and t' , according to $\langle \Delta r_i^2(t) \rangle = \langle [x_i(t+t') - x_i(t)]^2 + [y_i(t+t') - y_i(t)]^2 \rangle_{t'}$. The ensemble-averaged mean-squared displacement (MSD), $\langle \Delta r^2(t) \rangle$, was calculated as the average of the time-averaged MSDs over all beads i in the sample. The ensemble-averaged MSD is the relevant quantity that allows us to extract the rheological properties of the material from the Brownian motion of the beads [18, 19, 28].

In a purely viscous fluid of viscosity η , such as water or glycerol, the Brownian motion of the probes is diffusive. This means that the ensemble-averaged MSD linearly increases with time, according to $\langle \Delta r^2(t) \rangle = 4Dt$ (in two dimensions), where D is the diffusion coefficient. In this simple case, the viscosity η can be estimated using the Stokes–Einstein relation, $\eta = kT/6\pi RD$, where R is the bead radius and kT is the thermal energy [28]. A number of soft materials (foams, colloids, gels), however, display more complex rheological properties than simple fluids. This is the case for viscoelastic fluids which are both viscous and elastic on the time scale at which they are probed. In that case, the ensemble-averaged MSD adopts a dependence that is no longer linear with time, which is a signature of the fact that the probed material is viscoelastic. In such cases, a generalized Stokes-Einstein equation will be used to determine the elastic and viscous moduli of the probed material [18, 19, 29].

III. RESULTS AND DISCUSSION

A. Plasma viscosity in sealed and open geometry

Plasma droplets viscosity was measured in open and sealed geometry as a function of waiting time t_w – the time since the droplet was deposited on the substrate. Fig. 2(A-E) shows the MSD for each bead in the sample (grey symbols), as well as the ensemble-averaged MSD (average over all beads in the sample, coloured symbols), as a function of waiting time t_w , at a temperature 15°C . In both geometries and at any t_w , the ensemble-averaged MSD

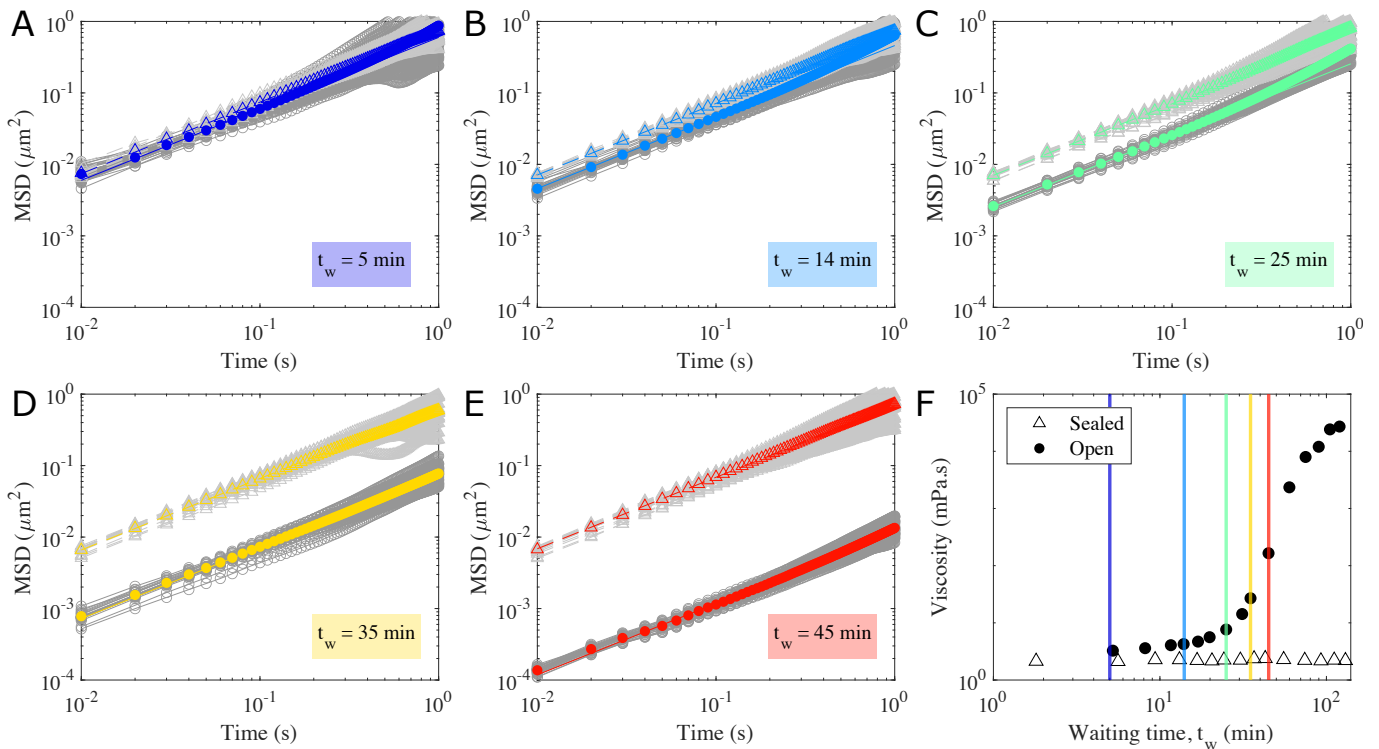


Figure 2. Plasma viscosity in the sealed and open geometry. (A-E). Mean-squared displacement (MSD) of micrometric melamine beads ($0.88 \mu\text{m}$ in diameter) in a plasma drop, in open (\bullet) and sealed (\triangle) geometry, at waiting times $t_w = 5$ min, $t_w = 15$ min, $t_w = 25$ min, $t_w = 35$ min and $t_w = 45$ min. The temperature was set at 15°C . The grey symbols correspond to individual beads, while the coloured symbols correspond to the average of all beads in the sample (17 – 33 beads depending on the realisation). In both geometries and at any t_w , the ensemble-averaged MSD is linear with time, indicating that the plasma is a purely viscous liquid. (F). Viscosity versus waiting time in both geometries, at 15°C . In the open geometry, the viscosity increases by 4 – 5 orders of magnitude over a hundred minutes, while it remains constant in the sealed geometry. The coloured vertical lines correspond to the different times t_w in graphs (A-E).

was linear with time. This indicates that the plasma is a purely viscous fluid, and can be described by a single parameter, the viscosity η . From the ensemble-averaged MSDs in Figs 2(A-E), we extracted a diffusion coefficient D , according to $\langle \Delta r^2(t) \rangle = 4Dt$, and then a viscosity η inversely proportional to D , according to the Stokes-Einstein relation [28]. Fig. 2F shows the viscosity in the two geometries as a function of the waiting time t_w . While remaining constant in the sealed geometry, the viscosity increased by 4 – 5 orders of magnitude over a hundred minutes in the open geometry, where water evaporation takes place. A close examination of our MSD data shows that the plasma remains a spatially homogeneous fluid at the bead scale – with or without evaporation – as demonstrated by the fact that the different beads in the sample (grey symbols) lead to a similar time-dependence of the MSD for each t_w and geometry.

B. Temperature dependence of viscosity

Plasma viscosity was first measured in the sealed geometry between 12.5°C and 32.5°C . The temperature dependence is shown in Fig. 3A where the viscosity is plotted as a function of the inverse temperature $1/T$. For comparison, viscosity data in hornworm plasma obtained with standard rheology [1], as well as tabulated viscosity-temperature data in water [30], are reported. The plasma viscosity of the bumblebee was higher than that of the hornworm and that of water. It decreased by a factor of 2 per temperature increase between 12.5°C and 32.5°C . The temperature dependence of viscosity could be described using a classical Arrhenius model for viscous fluids, $\eta(T) = \eta_\infty \exp(E_a/RT)$, where η_∞ is a reference viscosity, R is the gas constant per mole ($8.34 \text{ J}\cdot\text{mol}^{-1}\cdot\text{K}^{-1}$) and E_a is the Arrhenius activation energy [31–33]. For the bumblebee plasma, the activation energy was estimated to be $E_a = 22.1 \pm 1.1 \text{ kJ}\cdot\text{mol}^{-1}$, comparable to, although larger than estimated in the hornworm larvae plasma, $E_a = 18.2 \pm 2.2 \text{ kJ}\cdot\text{mol}^{-1}$, from the data of Kenny *et al.* [1]. The E_a was estimated to be $18.0 \pm 1.1 \text{ kJ}\cdot\text{mol}^{-1}$, lower than that obtained for insects. This

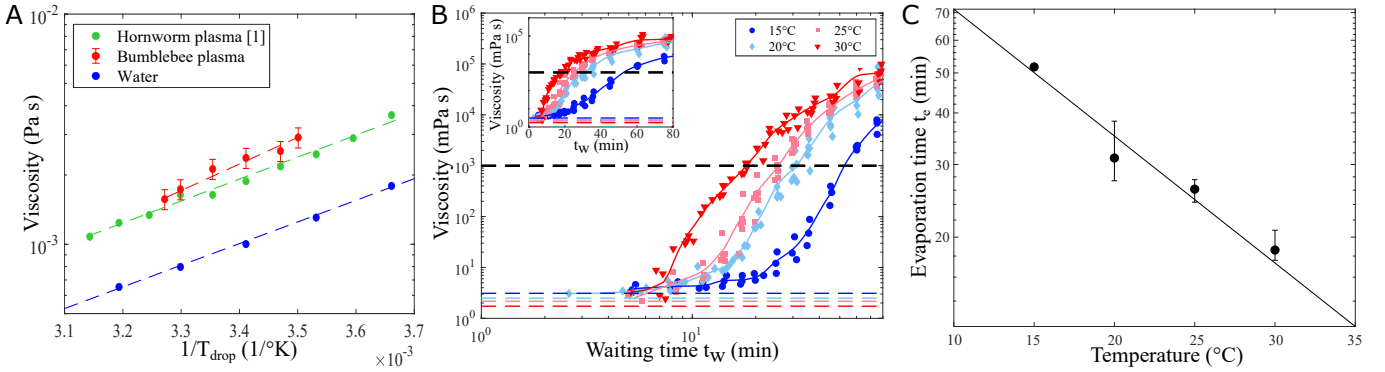


Figure 3. Temperature dependence of viscosity. (A). Viscosity of bumblebee plasma in sealed geometry (red dots) as a function of inverse temperature. For comparison, viscosity is also shown for water [30] and hornworm plasma [1]. The dashed lines represent the respective fit according to Arrhenius law. (B). Viscosity of bumblebee plasma in open geometry in the range 15–30°C as a function of waiting time (the inset shows a log-linear plot of the data). The constant viscosity values obtained in the sealed geometry for the same temperatures have been added (horizontal dashed coloured lines). Five experiments were performed per temperature, except at 15°C, where 3 experiments were performed. (C). Characteristic evaporation time t_e , defined for a viscosity of 1 Pa s (black dashed horizontal line in graph B), as a function of temperature. Evaporation time decreases with temperature, according to $t_e = t_0 \exp(-T/T_1)$, where $t_0 = 144.9$ min and $T_1 = 14.1^\circ\text{C}$ (solid line).

is consistent with the fact that insect plasma is composed of 90% water, but also other components such as highly soluble organic and inorganic constituents. It is interesting here to consider that the difference between the activation energies of the insect plasmas is related to their difference in composition, and is a signature of the species considered.

Fig. 3B shows the evaporation dynamics of the bumblebee plasma – viscosity versus waiting time – between 15°C and 30°C. We measured a significant increase in viscosity of 4 to 5 orders of magnitude over the duration of the experiment, typically 1 hour. Evaporation, and thus viscosity increase, accelerates with temperature. At the end of each experiment, when the viscosity reached 10^4 to 10^5 Pa s, the material was so viscous that the Brownian motion of the beads could not be detected because it was below the resolution limit of the experimental device (camera and objective). A characteristic evaporation time t_e was defined for a viscosity of 1 Pa s which corresponds to an increase of 3 orders of magnitude (1000 times the viscosity of water). We estimated that the evaporation time decreases with temperature, according to the empirical law $t_e = t_0 \exp(-T/T_1)$, where $t_0 = 144.9$ min and $T_1 = 14.1^\circ\text{C}$, as shown in Fig. 3C. The slow evaporation of plasma highlights the role of its constituents – proteins, amino acids – in the process. While a drop of pure water of the same volume would evaporate in about ten minutes at 25°C, the drop of plasma showed an increased viscosity for more than 1 hour while maintaining a large volume (typical humidity of 30%).

IV. CONCLUSION

The aim of this study was to present a methodology for measuring the rheology of biological fluids available in small quantities, such as bumblebee plasma, using a particle tracking microrheology technique. We describe the impact of temperature on the rheology of plasma in a sealed geometry and show that the plasma viscosity follows an Arrhenius law at temperatures between 12.5 and 32.5°C. The activation energy is comparable to that of the hornworm larvae measured in a standard cone-plane viscometer, by Kenny *et al.*[1], which requires relatively large samples of the order of 0.7 mL. Our rheological measurements with particle tracking microrheology show that plasma is a purely viscous fluid. This is consistent with the fact that it is composed of 90% water. It also contains numerous compounds such as amino acids and proteins [3, 4], which are insect-dependent and are expected to have an impact on the activation energy. An interesting point here is that the difference between the activation energies of the insect plasmas is certainly related to the difference in their composition and could be considered a signature of the species in question. In the open geometry, evaporation of water in the plasma caused the viscosity to increase by 4–5 orders of magnitude. Depending on the temperature, the time scale of evaporation ranged from tens of minutes to 1 h. These time scales are much longer than those that characterise coagulation, a mechanism that protects the insect from dehydration and pathogens by triggering a coagulation cascade that forms a seal. One might think that the slow evaporation of plasma maintains the integrity of the fluid that suspends the blood cells and proteins involved in clotting, allowing it to happen. Our experiments were carried out with 2–3 μl of sample, which is well suited to medium-sized insects. Fluid quantities in the tens of picoliter can also be considered, provided that the fluid of interest can be collected

or extracted. These experiments pave the way for new measurements of viscosity in insects, for a more detailed characterisation.

ACKNOWLEDGEMENTS

This project has received funding from the Clean Sky 2 Joint Undertaking (JU) under grant agreement No 864769. The JU receives support from the European Union’s Horizon 2020 Research and Innovation program and the Clean Sky 2 JU members other than the Union. BM was funded by a postdoctoral fellowship from FRS-FNRS (Fonds de la Recherche Scientifique).

COMPETING INTERESTS

The authors declare no competing or financial interests.

AUTHOR CONTRIBUTIONS

Conceptualization: A.L., J.B., B.A.; Methodology: A.L., B.M., V.T., O.S., J.B., B.A.; Software: B.A.; Validation: A.L., B.M., V.T., O.S., J.B., B.A.; Formal analysis: A.L.; Investigation: A.L., J.B., B.A.; Resources: B.A.; Data curation: A.L.; Writing - original draft: A.L., J.B., B.A., B.M.; Writing - review & editing: A.L., J.B., B.A.; Visualization: A.L., J.B., B.A.; Supervision: J.B., B.A.; Project administration: J.B., B.A.; Funding acquisition: J.B., B.A.

FUNDING

This project received funding from the Clean Sky 2 Joint Undertaking (JU) under grant agreement no. 864769. The JU receives support from the European Union’s Horizon 2020 Research and Innovation program and the Clean Sky 2 JU members other than the Union. B.M. was funded by a postdoctoral fellowship from FRS-FNRS (Fonds de la Recherche Scientifique).

DATA AVAILABILITY

All relevant data can be found within the article and its supplementary information.

-
- [1] M. Kenny, M. N. Giarra, E. Granata, and J. J. Socha, *Journal of Experimental Biology* **221**, jeb186338 (2018).
 - [2] M. I. Siddiqui and M. S. Al-Khalifa, *Italian Journal of Zoology* **81**, 2 (2014).
 - [3] G. R. Wyatt, *Annual Review of Entomology* **6**, 75 (1961).
 - [4] R. F. Chapman, S. J. Simpson, and A. E. Douglas, *The Insects Structure and Function* (5th Edition, 2013).
 - [5] Kanost, “Encyclopedia of insects (second edition),” (Elsevier, 2009) Chap. Hemolymph.
 - [6] J. F. Hillyer and G. Pass, *Annual Review of Entomology* **65**, 121 (2020).
 - [7] J. L. Nation, *Insect physiology and biochemistry* (3rd ed. Florida: CRC Press, 2016) p. 420–4.
 - [8] G. Bidla, M. Lindgren, U. Theopold, and M. S. Dushay, *Developmental & Comparative Immunology* **29**, 669 (2005).
 - [9] U. Theopold, O. Schmidt, K. Söderhäll, and M. S. Dushay, *Trends in immunology* **25**, 289 (2004).
 - [10] B. Heinrich, *Endeavour* **19**, 28 (1995).
 - [11] C. A. Halsch, A. M. Shapiro, J. A. Fordyce, C. Nice, J. H. Thorne, D. P. Waetjen, and M. L. Forister, *PNAS* **12**, 118 (2021).
 - [12] A. Liebhold and B. Bentz, US Department of Agriculture, Forest Service, Climate Change Resource Center (2011).
 - [13] C. Robinet and A. Roques, *Integrative Zoology* **5**, 132 (2010).
 - [14] J. D. Burdine and K. E. McCluney, *Scientific Reports* **9**, 1 (2019).
 - [15] S. L. Chown, J. G. Sørensen, and J. S. Terblanche, *Journal of insect physiology* **57**, 1070 (2011).
 - [16] H. Tabunoki, N. T. Dittmer, M. J. Gorman, and M. R. Kanost, *BMC Research Notes* **12**, 2 (2019).
 - [17] P. Aprelev, T. F. Bruce, C. E. Beard, P. H. Adler, and K. G. Kornev, *Scientific Reports* **9**, 3451 (2019).

- [18] T. A. Waigh, Rep. Prog. Phys **68**, 685 (2005).
- [19] T. A. Waigh, Rep. Prog. Phys **79**, 074601 (2016).
- [20] B. Abou, C. Gay, B. Laurent, O. Cardoso, D. Voigt, H. Peisker, and S. Gorb, Journal of The Royal Society Interface **7**, 1745 (2010).
- [21] P. Sprenger, L. H. Burkert, B. Abou, W. Federle, and F. Menzel, Journal of Experimental Biology **221**, jeb171488 (2018).
- [22] F. Menzel, S. Morsbach, J. H. Martens, P. Räder, S. Hadjaje, M. Poizat, and B. Abou, Journal of Experimental Biology **222**, jeb210807 (2019).
- [23] B. Heinrich, *Bumblebee economics* (Harvard University Press, 2004).
- [24] P. Soroye, T. Newbold, and J. Kerr, Science **367**, 685 (2020).
- [25] B. Martinet, S. Dellicour, G. Ghisbain, K. Przybyla, E. Zambra, T. Lecocq, M. Boustani, R. Baghirov, D. Michez, and P. Rasmont, Conservation Biology **35**, 1507 (2021).
- [26] K. Arafah, S. N. Voisin, V. Masson, C. Alaux, Y. Le Conte, M. Bocquet, and P. Bulet, Proteomics **19**, 1900268 (2019).
- [27] W. Rasband, ImageJ, U. S. National Institutes of Health, Bethesda, Maryland, USA, (1997-2018), <https://imagej.nih.gov/ij/>.
- [28] A. Einstein, Ann. Phys. **322**, 549 (1905).
- [29] T. Mason, Rheol. Acta **39**, 371 (2000).
- [30] J. Rumble, *CRC Handbook of Chemistry and Physics* (CRC Press, 2021).
- [31] J. De Guzmán, Anales de la Sociedad Espanola de Fisica y Quimica **11**, 353 (1913).
- [32] H. Eyring, J. Chem. Phys. **3**, 107 (1935).
- [33] H. Eyring, J. Chem. Phys. **4**, 283 (1936).